Research of Pattern Formation, edited by R. Takaki, pp. 205–215.

Various Growing Modes of Crystal in Diffusion Field

Haruo HONJO

College of General Education, Kyushu University,
Ropponmatsu, Fukuoka 810, Japan

Abstract. We review the experimental phase diagram of growing crystal patterns for succinonitrile in a supercooling-anisotropy phase space. The anisotropy of the crystal growth system is changed and various growing modes are observed. We discuss the degree of the anisotropy of the growing modes and the relation between regular dendrite and diffusion-limited aggregation.

1. Introduction

We have investigated the pattern formation in the diffusion field; dendrite (Honjo and Sawada, 1982; Honjo *et al.*, 1985) and DLA (diffusion-limited-aggregation; Matsushita *et al.*, 1984; Honjo *et al.*, 1986, 1987; Ohta and Honjo, 1988). The dendrite is a regular pattern with side-branches and DLA is an irregular one with tip-splitting phenomenon. The researches about them has been done with simulations, theories and experiments in crystal growth, fluid dynamical system, electrical chemical deposit system and so on (Pelce, 1981; Stanley and Ostrowsky, 1985). The important parameter discriminating dendrite and DLA is the degree of anisotropy of the system. The dendrite needs a non-zero anisotropy and DLA has no anisotropy.

We report the importance of the anisotropy of growing crystal and show the phase diagram of growing patterns of succinonitrile in a supercooling-anisotropy phase space. The growing patterns exhibit various growing behaviors such as tip-splitting, tip-oscillating and tip-stable modes.

2. Experiment

At the fixed supercooling in a melt growth system, the growing crystal has a determined pattern. That is, the crystal form depends on supercooling and the form at high supercooling is usually observed as a dendrite. Then, in order to observe various growing forms at the fixed supercooling, we need to introduce the degree of anisotropy to the crystal-growing system.

In Fig. 1 we show the experimental setup. The crystal cell is made quasi two dimensionally and the thickness of the spacer d is 14 μm. The thin bottom glass whose thickness is about 0.3 μm is scratched randomly by abrasives (the characteristic length of the roughness is l (μm)) and attached to a sapphire glass. The roughness l means that the two dimensional (horizontal) roughness is of order l. The value of l is determined from the image analysis (two dimensional Fourier spectrum analysis) of the pictures of roughened glass. It is expected that the glass is roughened vertically by the same order. This glass is pasted on a current-conductive glass and the temperature of this system is controlled by the current through the bridge circuit. The accuracy of the controlled temperature is ±0.025°C. Succinonitrile is sealed in this thin cell. Succinonitrile is a transparent plastic crystal at room temperature and has four-fold symmetry. The pictures of growing crystals are taken using a video tape recorder through a microscope and a TV camera, and then processed by the image analysis technique.

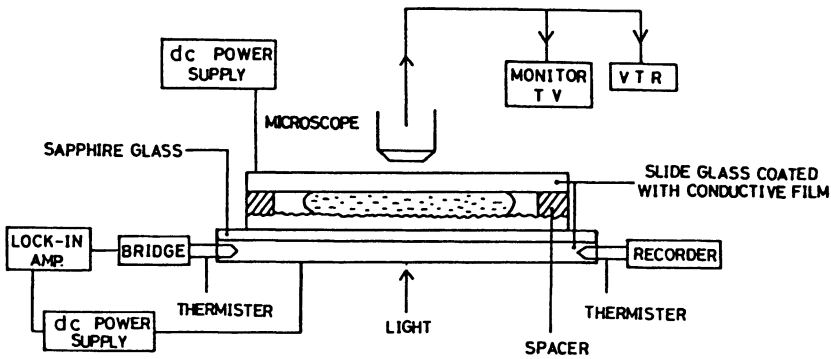

Fig. 1. The experimental setup. Succinonitrile is sealed in the quasi-two-dimensional cell whose bottom glass is roughened randomly. The pictures are taken using a video tape recorder.

A crystalline anisotropy is originally determined microscopically as the strength of bonding between atmos and its value is constant. However, as long as we pay attention to the macroscopic growing pattern and its growth direction under the perturbations, we can introduce a as the growth directional anisotropy of the

pattern.

Let us define a by $\alpha \equiv d/l$ considering the geometry of the cell. This definition results from the estimation as follows. In the case of $l << l_c$, l_c is the characteristic length of the crystal such as the tip radius of curvature, a is much stronger because very small-sized perturbations are averaged out to yield no influence to the crystal tip stronger, and when $l \sim l_c$, the tip is influenced very strongly by the roughness. Furthermore, d enhances the above effect considering the vertical geometry of the cell. As we will show later, the growth behavior depends on both supercooling and α. We change the roughness by the three cases l = 34, 16 and 10 μm. These values are averaged ones and each variance of the roughness is about $\pm l/2$.

The thermal conductivities liquid succinonitrile at melting point and the roughened glass are $k_{su} = 5.32 \times 10^{-4}$ cal/cm·s·k (Glicksman *et al.*, 1977) and $k_{gl} = 1.44 \times 10^{-3}$ cal/cm·s·k ($= 2.7\, k_{su}$), respectively. The crystal tends to grow toward the protrusions on the surface of the randomly roughened glass, which give random perturbations to the crystal tip. The succinonitrile is first crystallized and then melted until only one small seed is left. We vary the supercooling temperature $\Delta\theta$ ($= T_M - T_\infty$) at any fixed a to make a phase diagram. Here T_M is the melting point of succinonitrile (= 54.5°C) and T_∞ is the temperature of the system. Our system of melt growth is three dimensional in thermal diffusion.

3. Results

Let us survey the typical growing patterns according to $\Delta\theta$ in the case of α = 0.875. For smaller $\Delta\theta$ (0.44°C), the growing mode is tip splitting (Fig. 2(a)). We also show a schematic picture in Fig. 2(b). The tip curvature and velocity oscillate, and the growth direction also oscillates. The preferred growth direction is <100>. One can see two sharp protrusions A and B in Figs. 2(a) and 2(b). A is in fresher liquid than B and grows as the tip. The position of B grows slowly to another direction as a sidebranch. This phenomenon is observed as tip splitting.

Because the growth direction of the tip A is not originally prefered, the tip velocity is decelerated and the tip curvature becomes smaller, and the growth direction recovers to <100>. On that occasion, there remains a protrusion C (Figs. 2(a) and 2(b)), which grows as a sidebranch. Consequently, this sidebranch C is asymmetric with the tip-splitted sidebranch B, and does not develop well because the supercooling there is reduced by the heat diffused from the tip. The global pattern is observed as follows. The tip-splitted sidebranches are well developed, while those on another side do not grow so well, and sidebranches of both sides are asymmetric. We call this growth mode the asymmetric tip-splitting (ATS) mode.

When $\Delta\theta$ is larger (1.99°C), the growing mode is still tip splitting (Fig. 3). The growth mechanism is the same as seen in Fig. 2. However, because of the larger supercooling, the two sharp protrusions can grow together as tips. After the tip-splitting, each tip grows with ATS mode because the distance between the two tips is close and the local supercooling around there is smaller. After the tips grow far

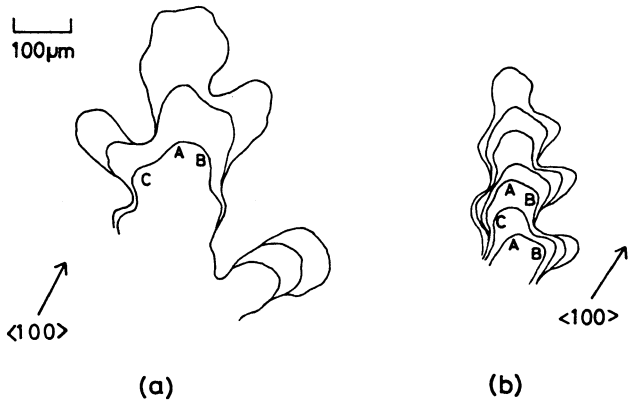

Fig. 2(a) Growing patterns overlapped in arbitrary time interval in the case of small $\Delta\theta$ (= 0.44°C). A is th etip, B grows as a well-developed sidebranch, and C grows as a less-developed one. The growing behavior is the asymmetric tip-splitting(ATS) mode.

Fig. 2(b). Overlapped schematic picture of Fig. 2(a). A, B and C are the same with Fig. 2(a).

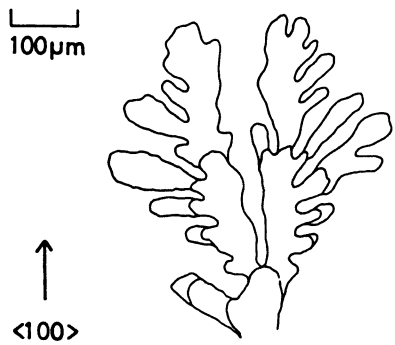

Fig. 3. Arbitrary overlapped growing patterns in the case of large $\Delta\theta$ (= 1.99°C). The characteristic length is smaller than that in the case of Fig. 2(a) and the growing behavior is the symmetric tip-splitting (STS) mode.

apart from each other, they repeat again the above tip-splitting. This growth mode is characterized as the simultaneous growth of the two splitted tips. Let us call this mode symmetric tip-splitting (STS) mode.

When $\Delta\theta$ is increased more (2.44°C), the tip-splitting cannot occur any more (Fig. 4(a)). The tip radius is smaller, and becomes more stable than former cases. The averaged growth direction is <100>. The disturbance from the rough surface of the cell brings about the tip oscillation, which causes asymmetric side branching.

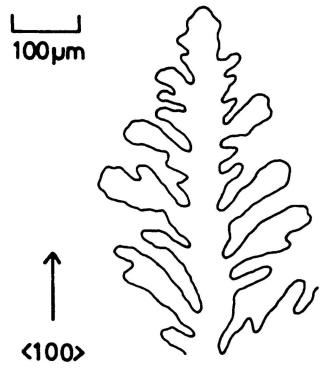

Fig. 4. The case of very large $\Delta\theta$ (= 2.44°C). The tip grows with oscillation and tip-splitting cannot occur. The growing behavior is the TO mode.

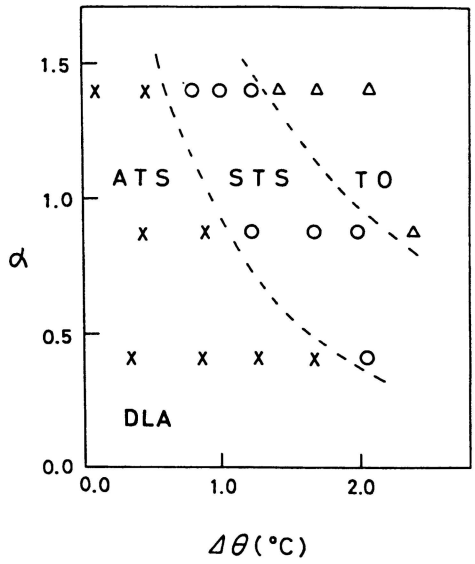

Fig. 5. Phase diagram of growing patterns in supercooling-anisotropy phase space. α is the anisotropy defined from the geometry of the cell. The tip-splitting and tip-oscillating modes are divided by the condition $\rho \sim l$. The DLA mode exists in lower α and $\Delta\theta$. A usual dendrite (TS mode) exists above the TO mode.

Although the asymmetry of sidebranches is not clear in this figure, we can identify it from the tip-oscillating growth in NH_4Cl solution. We call this mode the tip-oscillating (TO) mode.

When $\Delta\theta$ is much larger, the tip is very stable and the roughness causes much less influence to the tip. The tip may grow in a stationary manner without oscillation, and the usual dendrite in a free space may be observed. However, this decision is difficult because the tip grows too fast. The stable tip forms a parabolic one, then we call this mode the stable parabolic-tip (SPT) mode.

In Fig. 5, we show the phase diagram of growing patterns for three values of the growth directional anisotropy α. With the increase of supercooling (or anisotropy) at the fixed anisotropy (supercooling), the pattern changes from ATS to STS and then to TO. The coexisting characteristic in these modes is tip-oscillation behavior. For smaller anisotropy, the tip-splitting modes are added, and for larger anisotropy the tip-oscillation is dominant.

4. Discussion

We discuss the growing situation with the various modes comparing the characteristic length (L μm) and the roughness (l μm).

In the case of $L >> l$ (ATS mode), we show the schematic figure of the crystal in Fig. 6(a). There exist the small perturbations of the thermal diffuse at the interface of the crystal because k_{gl} is larger than k_{su}. By the theoretical results of dendrite (Langer, 1980), the temperature of the interface T_{int} is determined by the Gibbs-Thomson's condition which depends on the curvature of interface and the anisotropy of the crystal. When T_{int} does not depend on the curvature and the anisotropy, that is, it is constant ($= T_M$; melting point), the interface has all of the solution of parabola (Ivantsov solution, Ivantsov, 1947) and the interface is unstable. In Fig. 6(a), in spite of $L >> l$, the roughness does not directly instabilize the interface with the scall of roughness. Then, the roughness diffuses the latent heat at random direction and

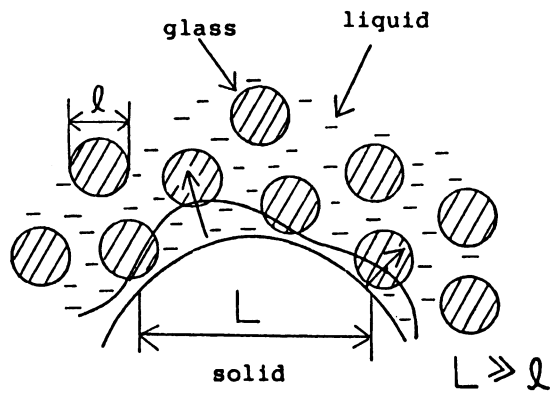

Fig. 6(a). Schematic figure around the crystal in the case of $L >> l$. L is the characteristic length of crystal and l is the one of roughness. This figure corresponds to ATS mode of Fig. 2.

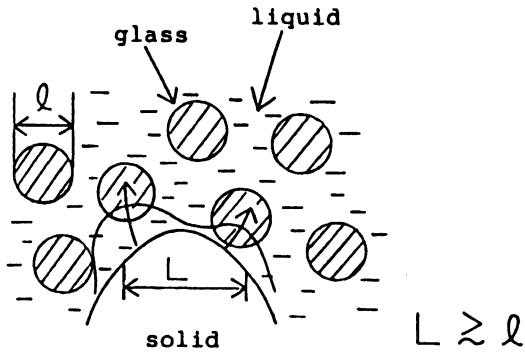

Fig. 6(b). Schematic figure around the crystal in the case of $L > l$. This figure corresponds to STS mode of Fig. 3.

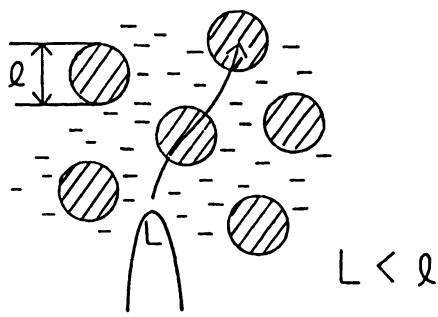

Fig. 6(c). Schematic figure around the crystal in the case of $L < l$. This figure corresponds to TO mode of Fig. 4.

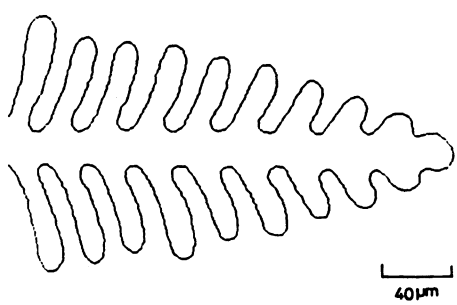

Fig. 6(d). Tip-oscillating growth of NH_4Cl dendrite. There exists a facet at the tip, which appears and disappears.

tends to make T_{int} constant. This may be reasonable considering that at the supercooling of this case, the tip of dendrite in a free space is a stable parabola. In other words, the roughness decreases the anisotropy of the growth direction, and the degree of the anisotropy of this case is much less. The number of unstable modes is at most two, which means the tip is splitted, because the supercooling is less.

In Fig. 6(b), we show the schematic figure of STS mode ($L > l$). The $\Delta\theta$ is larger than the one of ATS mode. L is smaller and the number of unstable mode is larger. Then the unstable modes can grow together as tips. This growing mode repeats tip-splitting and fills the two dimensional space. The global pattern may correspond to the dense-radial pattern which is reported in electro chemical deposit (Grier *et al.*, 1987). This pattern is observed in the case of relatively small anisotropy, that is, in the intermediate region among DLA and dendrite. There are mixed both the preferred direction of the crystal and the tip-splitted direction. In Photo. 1, we also show the photograph of the dense-radial pattern of NH_4Cl crystal in the solution growth system. There coexist the directions of <100> and <110> with repeating tip-splitting. The detail mechanism about dense-radial pattern is an open question.

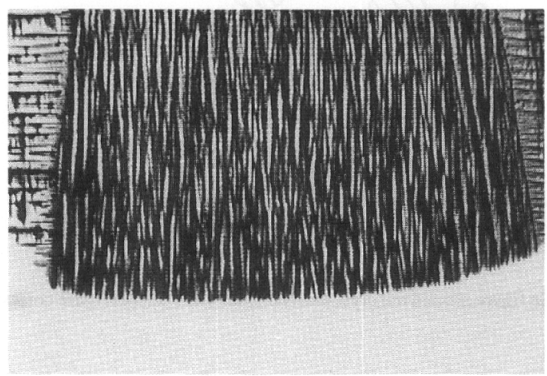

Photo. 1. Dense-radial pattern growing in a supersaturated NH_4Cl solution in a two-dimensional growth cell.

In Fig. 6(c), we show the schematic figure of the case of much larger $\Delta\theta$ ($L < l$). The tip is influenced by the roughness then the tip-splitting does not occur but oscillates toward the protusions of glass. The global pattern is similar to the one observed in a free space setting aside the tip-oscillating. We can observe the tip-oscillating growth in the NH_4Cl solution in a two-dimensional space(Fig. 6(d)). In this case, there exists an impurity in the solution and the facet at the one side of the tip appears and disappears. This oscillation produces the asymmetric sidebranches. However, the top of the dendrite does not usually oscillate and is a stable parabola.

The oscillating growth needs another condition, e.g., impurity or roughness, which works as changing the anisotropy. The Gibbs-Thomson's boundary condition is considered to be achieved in the thermal large perturbation (l).

Let us estimate the order of the characteristic length of our pattern l_c (Fig. 4). The averaged velocity is v = 500 μm/s, the diffusion constant $D = 1.16 \times 10^{-3}$ cm^2/s. Hence, the diffusion length is $l_d \equiv 2D/v = 460$ μm. The surface tension is $\gamma = 2.14 \times 10^{-7}$ cal/cm^2, the latent heat L = 885.1 cal/mol, the specific heat $c_p = 38.25$ cal/mol·K, and the melting point $T_M = 327.65$ K, so the capillary length is $d_o \equiv \gamma T_M c_p / L^2 = 27$ A°. From the Langer-Muller-Krumbhaar (LMK) theory (Langer and Muller-Krumbhaar, 1978a, 1978b, 1978c) the characteristic length without roughness $l_{co} = \rho = (l_d d_o/\sigma^*)^{1/2} = 7$ μm. Here ρ is the tip radius of curvature and $\sigma^* = 0.0025$ in three dimensions. From Fig. 4, $\rho \sim 7$ μm, which agrees with the above result. Strictly speaking, the tip in the LMK theory is stable, while the tip Fig. 4 is oscillating. Nevertheless, we can roughly estimate l_c from the LMK theory. From the late analysis considering the crystalline anisotropy of the needle crystal in a fully nonlocal model (Barbieri *et al.*, 1987), σ^* is rewritten as $\sigma_o \alpha_d^{7/4}$ in two dimensions. Here σ_o is of order unity and α_d is the degree of the anisotropy in capillary length (surface tension).

From the geometry of the cell, we have defined α as d/l. This definition corresponds to that of Ben-Jacob *et al.* (1985) and neglects the effect of l_c on α. On the other hand, the nondimensional parameter B of the simulation by Liang (1986) is defined as L_{VF}^2/W_{VF}^2. Here L_{VF} is the characteristic length of viscous fingering and W_{VF} is the width of Hele-Shaw cell. B represents the influence of the wall on the finger width, i.e., the effective one-dimensional anisotropy. In our system, a larger l_c (smaller Δθ) tends to make the tip more unstable (tip splitting). On the other hand, we can phenomenologically recognize that the tip splitting occurs because of weaker anisotropy. Therefore, we can suppose the real growth directional anisotropy experienced by the tip as α, and it is considered a decreasing function of l_c. l_c is larger than l_{co} because the roughness weakens α. Couder, Gerard and Rabaud (1986) showed experimentally that the width of a viscous finger whose tip has a bubble, which increases the anisotropy, is smaller than the one without a bubble. The above discussion about the relation between α and l_c qualitatively explains their results.

Moreover, α is an increasing function of the degree of the crystalline anisotropy ε, d/l, and k_{su}/k_{gl}. Here, the strength of thermal perturbations in our system is k_{gl}/k_{su}, which leads to the above effect on α. Therefore, the variations of growing behaviors in our system can be recognized as the results of the competition between the destabilizing factor l_c and the stabilizing factors ε, d/l and k_{su}/k_{gl} (Fig. 5).

There seems to exist a critical value of characteristic length l_c^*, which separates the tip-splitting mode and the tip-oscillating mode when l is constant. From Figs. 3 and 5, l_c^* exists in the vicinity of the supercooling region of Fig. 3. When the symmetric tip splitting occurs in Fig. 3 the tip radius of curvature $\rho^* = l_c^* \sim l$ (16 μm). This leads to the result that if l_c is smaller than the spacial scale of mac-

roscopic thermal fluctuations (l), the crystal tip grows to the thermally favorable direction with oscillation rather than with tip splitting. The transition from one growing mode to another seems to be continuous in our system. This results from the variance of roughness. If a subtle experiment without the variance of roughness is devised, the transition between growing modes may be discontinuous.

A DLA growth takes place through repeating the tip splitting irregularly, and this phenomenon corresponds to the ATS and STS modes. The STS mode clearly shows the crystalline anisotropy <100> direction because ~ is larger. We conjecture that there exists the DLA mode in the region where ~ is very small, i.e., α is small and l_c is large in the ATS mode (Fig. 5). A pattern with nonzero but small anisotropy in DLA simulations yields the isotropic DLA mode until some cluster size (Meakin, 1986). The related discussion may be possible for the ATS and STS modes in the crystal growth and we will continue experimental investigations on the subjects.

REFERENCES

Barbier, A., Hong, D. C.,and Langer, J. S. (1987), Velocity selection in the symmetric model of dendritic crystal growth, Phys. Rev. A, **35**, 1802–1808.

Ben-Jacob, E., Godbey, R., Goldenfeld, N., Koplik, J., Levine, H., Mueller, T., and Sander, M. (1986), Experimental demonstration of the role of anisotropy in interfacial pattern formation, Phys. Rev. Lett., **55**, 1315–1318.

Couder, Y., Gerard, N., and Rabaud, M. (1986), Narrow fingers in the Saffman-Taylor instability Phys. Rev. A, **34**, 5175–5178.

Glicksman, M. E., Schaefer, R. J., and Ayers, J. D. (1976), Dendritic growth-a test of theory, Met. Trans. A, **7A**, 1747–1759.

Grier, D. G., Kessler, D. A., and Sander, L. M. (1987), Stability of the dense radial morphology in diffusive pattern formation, Phys. Rev. Lett., **59**, 2315–2318.

Honjo, H. and Sawada, Y. (1982) Quantitative measurements on the morphology of a NH_4Br dendritic crystal growth in a capillary, J. Crystal Growth **58**, 297–303.

Honjo, H., Ohta, S., and Sawada, Y. (1985), New experimental findings in two-dimensional dendritic crystal growth, Phys. Rev. Lett., **55**, 841–844.

Honjo, H., Ohta, S., and Matsushita, M. (1986), Irregular fractal-like crystal growth of ammonium chloride, J. Phys. Soc. Jpn, **55**, 2487–2490.

Honjo, H., Ohta, S., and Matsushita, M. (1987), Phase diagram of a growing succinonitrile crystal in supercooling-anisotropy phase diagram, Phys. Rev. A, **36**, 4555–4558.

Ivantsov, G. P. (1947), Temperature field around a spherical, cylindrical and acicular crystal growing in a supercooled melt, Doklady Akad. Nauk SSSR, **58**, 567–569.

Langer, J. S. (1980), Instabilities and pattern formation in crystal growth, Rev. Mod. Phys., **52**, 1–28.

Langer, J. S. and Muller-Krumbhaar, H. (1978), Theory of dendritic growth-I. Elements of a stability analysis, Acta Metall., **26**, 1681–1687.

Langer, J. S. and Muller-Krumbhaar, H. (1978), Theory of dendritic growth-II. Stabilities in the limit of vanishing surface tension, Acta Metall., **26**, 1689–1695.

Langer, J. S. and Muller-Krumbhaar, H. (1978), Theory of dendritic growth-III. Effects of surface tension, Acta Metall., **26**, 1697–1708.

Liang, S. (1986), Random-walk simulations of flow in Hele Shaw cells, Phys. Rev. A, **33**, 2663–2674.

Matsushita, M., Sano, M., Hayakawa, Y., Honjo, H., and Sawada, Y. (1984), Fractal structures of zinc metal leaves grown by electrodeposition, Phys. Rev. Lett., **53**, 286–289.

Meakin, P. (1986), Universality, nonuniversality, and the effects of anisotropy on diffusion-limited

aggregation, Phys. Rev. A, **33**, 3371–3382.
Ohta, S. and Honjo, H. (1988), Growth probability distribution in irregular fractal-like crystal growth of ammonium chloride, Phys. Rev. Lett., **60**, 611–614.
Pelce, P. (ed.) (1988), Dynamics of curved fronts, (Academic Press Inc.).
Stanley, H. E. and Ostrowsky, N. (ed.) (1985), On growth and Form, (Martinus Nijhoff).